Spectrochimica Acta Part A: Molecular and Biomolecular Spectroscopy 120 (2014) 332–339

Contents lists available at ScienceDirect

Spectrochimica Acta Part A: Molecular and Biomolecular Spectroscopy

journal homepage: www.elsevier.com/locate/saa

Evaluation of the anti-inflammatory and analgesic effects of Cu(II) and Zn(II) complexes derived from 2-(naphthalen-1-yloxy)-*N*′-(1-(pyridin-2-1)ethylidene) acetohydrazide

Ola A. El-Gammal [a,*], Elsayed A. Elmorsy [b,c], Yousery E. Sherif [c,d]

[a] Department of Chemistry, Faculty of Science, Mansoura University, Mansoura, P.O. Box 70, Mansoura, Egypt
[b] Pharmacology Department, Faculty of Medicine – North Jeddah Branch, King Abd El-Aziz University, Kingdom of Saudi Arabia
[c] Clinical Pharmacology Department, Faculty of Medicine, Mansoura University, Mansoura, Egypt
[d] Department of Chemistry, Faculty of Science and Arts, Ulla, Taibah University, Kingdom of Saudi Arabia

HIGHLIGHTS

- Preparation of complexes of 2-(naphthalen-1-yloxy)-*N*′-(1-(pyridin-2-yl)ethylidene) acetohydrazide (HA2PNA) with Zn and Cu acetate.
- Characterization of all compounds by elemental and spectral techniques.
- Anti-inflammatory and analgesic activity in rat model of collagen adjuvant arthritis and compared with piroxicam.

GRAPHICAL ABSTRACT

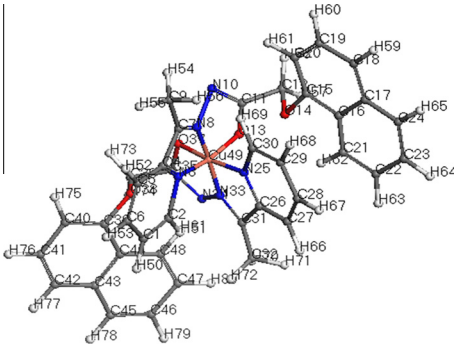

ARTICLE INFO

Article history:
Received 6 June 2013
Received in revised form 11 September 2013
Accepted 26 September 2013
Available online 10 October 2013

Keywords:
Anti-inflammatory
Analgesic
Acetohydrazide
Copper
Zinc

ABSTRACT

New Cu(II) and Zn(II) complexes of 2-(naphthalen-1-yloxy)-*N*′-(1-(pyridin-2-yl)ethylidene) acetohydrazide (HA2PNA) have been prepared and characterized by elemental analyses, spectral (IR, UV–visible, ESR and ^{1}H NMR) as well as magnetic and thermal measurements. According to the data, the complexes assigned the formulae: $[Cu(A2PNA)_2]H_2O$ and $[Zn(A2PNA)(OAc)(H_2O)]$, respectively. IR data revealed that the ligand acts as before ONN and after morever ONN mononegative tridentate via deprotonated carbonyl oxygen (=C—O—) and both $(C{=}N)_{imine}$ and $(C{=}N)_{pyridine}$ nitrogen atoms. The bond lengths, bond angles, HOMO, LUMO, dipole moment and charges on the atoms have been calculated by using density functional theory (DFT) at B3LYP level with 6-31G and 6-31G(d,p) basis sets to confirm the geometry of the ligand and the investigated complexes. Also, the kinetic parameters were determined for each thermal degradation stage of the complexes using Coats–Redfern and Horowitz–Metzger methods. Moreover, the complexes have been tested for anti-inflammatory and analgesic activity in rat model of collagen adjuvant arthritis and compared with piroxicam. All the compounds showed a significant anti-inflammatory and analgesic effect versus piroxicam.

Introduction

Rheumatoid arthritis (RA) is a chronic inflammatory disease characterized by joint swelling, joint tenderness and destruction of synovial joints, leading to severe disability and premature mortality [1]. Persistent high disease activity leads to disability, comor-

* Corresponding author. Tel.: +20 126712958.
E-mail address: olaelgammal@yahoo.com (O.A. El-Gammal).

1386-1425/$ - see front matter © 2013 Elsevier B.V. All rights reserved.
http://dx.doi.org/10.1016/j.saa.2013.09.067

bidities, and premature mortality. Consequently, development of treatment strategies to bring the disease under control quickly is of utmost importance [2]. Nonsteroidal anti-inflammatory drugs (NSAIDs) are among the most widely used therapeutics, primarily for the treatment of pain and inflammation, especially arthritis [3]. Piroxicam is a nonsteroidal anti-inflammatory drug and it has anti-inflammatory, analgesic and antipyretic activity [4]. The role of zinc and copper in chronic inflammatory diseases is of interest because they are co-factors of important enzymes involved in collagen and bone metabolism [5,6] immune system function [7,8] and antioxidant protection [9]. Furthermore, changes in serum zinc and copper levels observed in RA patients led some investigators to hypothesize that a marginal deficiency in zinc and copper might contribute to the development of RA and to the progression of the disease itself [10]. Also, it has been shown that the inflammation associated with rheumatoid arthritis can be reduced using copper complexes [11].Hydrazones are a versatile class of compounds which present innumerous chemical and pharmacological applications. They have shown to possess antimicrobial, anticonvulsant, analgestic, anti-inflammatory, antiplatelet, antitubercular, antitumoral properties [12–15]. Literature survey showed no pharmacological assay on the present hydrazone, 2-(naphthalen-1-yloxy)-*N*′-(1-(pyridin-2-yl)ethylidene) acetohydrazide (HA2PNA) has yet been undertaken. So, this work aims to study the anti-rhemuatic activity of the present hydrazone (HA2PNA) as well as its Cu(II) and Zn(II) complexes.

Experimental

Instrumentation and materials

All the chemicals were purchased from Aldrich and Fluka and used without further purification. Elemental analyses (C, H, N) were performed with a Perkin–Elmer 2400 series II analyzer. Molar conductance values (10^{-3} mol l^{-1}) of the complexes in DMF were measured using a Tacussel conductivity bridge model CD6NG. IR spectra (4000–400 cm^{-1}) for KBr discs were recorded on a Mattson 5000 FTIR spectrophotometer. Electronic spectra were recorded on a Unicam UV–visible spectrophotometer UV2. Magnetic susceptibilities were measured with a Sherwood scientific magnetic susceptibility balance at 298 K. ^{1}H NMR measurements in d6-DMSO at room temperature were carried out on a Varian Gemini WM-300 MHz spectrometer at the Microanalytical Unit, Cairo University. Thermogravimetric measurements (TGA, DTA, 20–1000 °C) were recorded on a DTG-50 Shimadzu thermogravimetric analyzer at a heating rate of 15 °C/min and nitrogen flow rate of 20 ml/min. A powder ESR spectrum was obtained in a 2 mm quartz capillary at room temperature with a Bruker EMX spectrometer working in the X-band (9.78 GHz) with 100 kHz modulation frequency. The microwave power and modulation amplitudes were set at 1 mW and 4G, respectively. The low field signal was obtained after four scans with 10-fold increase in the receiver again.

Synthesis of α-naphthoxyacetylhydrazine

α-naphthoxyacetylhydrazine was synthesized by the literature method [16]. A solution of ethyl α-naphthoxyacetate (23 ml, 0.1 mol) and 100 ml of absolute ethanol were added to 5.0 ml of hydrazine hydrate (0.1 mol) and the mixture was refluxed for 3 h. The obtained solution was evaporated to one third its original volume. Then the product formed was cooled, filtered off, washed several times with diethyl ether and finally dried over anhydrous $CaCl_2$; yield ≈16.2 gm; m.p: 158–160 °C.

Synthesisof2-(naphthalen-1-yloxy)-N′-(1-(pyridin-2-l)ethylidene)acetohydrazide(HA2PNA)

2-(naphthalen-1-yloxy)-*N*′-(1-(pyridin-2-yl)ethylidene)acetohydrazide (HA2PNA) was prepared by heating equimolar amounts of 2-acetylpyridine (11 ml, 0.1 mol) and α-naphthoxyacetylhydrazine (23.4 gm, 0.11 mol) in 150 ml absolute ethanol under reflux for 2 h. On cooling, piege precipitate was separated. The product was filtered off, washed, recrystallized from absolute ethanol and finally dried in a vacuum desiccator over anhydrous calcium chloride. Yield ≈25.4 gm, m.p. 180–183 °C.

Synthesis of metal complexes

A hot ethanolic or aqueous ethanolic solution of the respective metal acetate (1.0 mmol) was added to hot ethanolic solution of HA2PNA (0.296 g, 1.0 mmol). The resultant mixture was heated under reflux for 1 h. The precipitates that formed were filtered off, washed with ethanol followed by diethyl ether and dried in a vacuum desiccator over anhydrous $CaCl_2$. The physical and analytical data of the isolated complexes are listed in Table 1. The complexes are stable and readily soluble in DMF and DMSO. The values of molar conductivity of all complexes, lie in the range (5–7 ohm^{-1} cm^2 mol^{-1}) indicating their non-electrolytic nature [17].

Pharmacological test

Animals

Fourty eight Sprague–Dawley rats (200–250 g) were fed on a standard rat chow and water and labium. Animal care and experiments were performed in accordance with NIH guide to the care and use of laboratory animals. The local ethical committee approved the study. Rats were housed under similar standard laboratory conditions. The animals were divided into two main groups [non arthritic control (n = 6) and arthritic group (n = 42)]. In the arthritic group, all rats had been inoculated by the reagent of collagen adjuvant arthritis into the left paw pad. Rats which developed right paw arthritic manifestations after 45 days were divided into seven groups each group contained 6 rats as follow, arthritic control, piroxicam treated, zinc acetate treated, copper acetate treated, (HA2PNA) treated, $[Cu(A2PNA)_2]H_2O$ complex

Table 1
Analytical and physical data of HA2PNA and its metal complexes.

Compound empirical formula (F Wt)	Color	M.p. (°C)	% Found (Calcd.)				Yield (%)
			M	Cl	C	H	
(HA2PNA) $C_{19}H_{17}N_3O_2$ (296.33)	Grey	183	–	–	71.38 (71.46)	5.42 (5.37)	–
$[Zn(A2PNA)(OAc)(H_2O)]$ $ZnC_{21}H_{21}N_3O_5$ (460.76)	Grey	260	14.10 (14.19)	–	54.46 (54.74)	4.67 (4.59)	84
$[Cu(A2PNA)_2]H_2O$ $CuC_{38}H_{34}N_6O_5$ (718.14)	Dark green	260	8.46 (8.38)	–	63.79 (63.55)	4.88 (4.77)	88

treated and [Zn(A2PNA)(OAc)(H_2O)] complex treated groups. The compounds were given orally via gastric tube once daily in a dose which calculated according to Paget's table for seven days [18]. Most of the previous compounds are insoluble in water, thus it were suspended in 0.5% sodium carboxymethyl cellulose [SCMC] mg per 200 g of rat weight. This model of Collagen–Adjuvant Arthritis [19–21] is considered to be a representative of rheumatoid arthritis or ankylosing spondylitis in humans. Collagen II – Freund's adjuvant emulsion (0.1 ml) was injected intradermally into the left hind foot paw-pad of each rat (if no arthritis developed within four weeks, some of the animals were challenged by a second inoculation). After 45 days, the systemic arthritis developed in both hind paws [22].

Methods of measurement of joint inflammation and pain tolerance

Pain tolerance: measurement right paw pad pressure tolerance. This was determined for assessment of the analgesic activity of the used drugs; pressure was applied by the analgesimeter (Ugo Basile, Italy) on the rat pad of the right paw. The pressure was increased gradually (a certain number of grams per second until the rat either squeaks or tries to withdraw its limb). The force of pressure was continuously monitored by a pointer moving along a linear scale. Increased pressure tolerance of drug treated rats indicates analgesic activity of the administered drug [23,24]. This measurement of pressure tolerance was done at the 7th day of drug treatment (45 days after complete Freund's adjuvant injection).

Proximal joint (right ankle) mobilization tolerance (pain scoring). This was graded from one to four. Degree 1 corresponds to tolerance of complete flexion 90°; degrees two and three correspond to increasing degree of maltolerance according to a rat hind limb withdrawal, squeaking and when the flexion becomes painful. Degree 4 corresponds to squeaking with just initiation of flexion. Each of the six non-arthritic, non-treated rats had a score of one [23]. This measurement of mobilization tolerance was done at the 7th day of drug treatment (52 days after complete Freund's adjuvant injection).

Measurement of joint inflammation: right ankle periarticular edema scoring (rheumatoid index). Scoring was based on severity and extent of the erythema and edema of the periarticular tissue, and the enlargement, distortion or ankylosis of the joints. Its inflammation was graded from 1 to 4 [23]. Grading of 4 was when the joint was distorted and ankylosed, 3 when markedly enlarged, 2 when erythematous with edema, and 1 when normal [23]. Each of the six non-arthritic, non-treated rats had a score of 1. Right paw pad thickness and joint scoring were measured at the 7th day after starting drug treatment (45 days after complete Freund's adjuvant injection).

Molecular modeling. We performed cluster calculations using DMOL^3 program [25] in Materials Studio package [26], which is designed for the realization of large scale density functional theory (DFT) calculations. DFT semi-core pseudopods calculations (dspp) were performed with the double numerical basis sets plus polarization functional (DNP). The DNP basis sets are of comparable quality to 6-31G Gaussian basis sets [27]. Delley and Kessi showed that the DNP basis sets are more accurate than Gaussian basis sets of the same size [28]. The RPBE functional [29] is so far the best exchange–correlation functional [30], based on the generalized gradient approximation (GGA), is employed to take account of the exchanged correlation effects of electrons. The geometric optimization is performed without any symmetry restriction.

Results and discussion

The data of elemental analysis together with some physical properties of the complexes are summarized in Table 1.The stiochiometries of the coordination adducts established by elemental analysis are confirmed by weight loss determination.

Molecular modeling

The molecular structure along with atom numbering of HA2PNA and its metal complexes are shown in Structures (I–III).

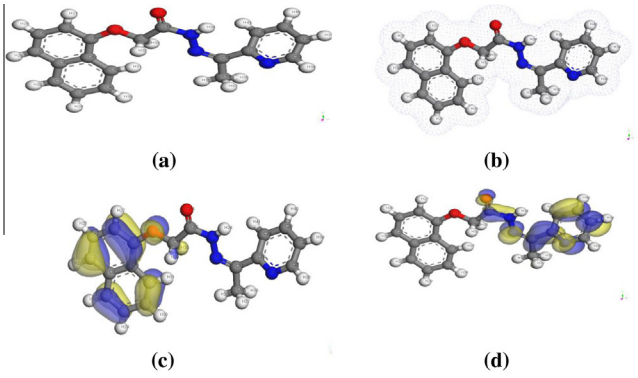

Structure I : molecular structure of (a) (HA2PNA) (b) electron density of (HA2PNA) (c) HOMO of (HA2PNA) (d) LUMO of (HA2PNA)

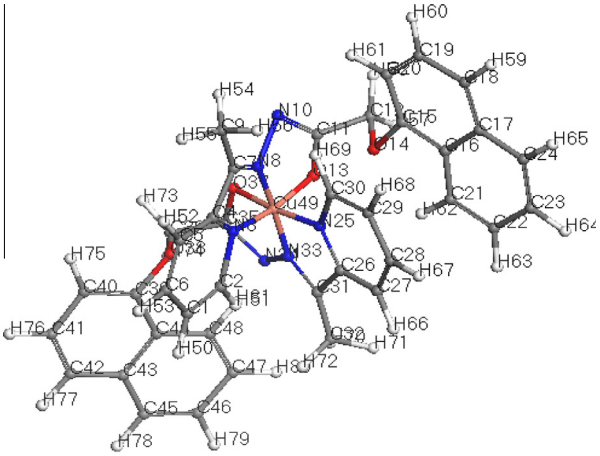

Structure II : molecular structure of [Cu(A2PNA)$_2$]H$_2$O

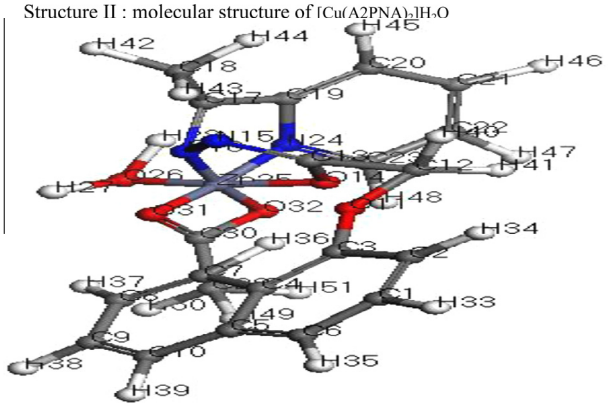

Structure II : molecular structure of [Zn(A_2PNA)(OAc)(H_2O)]

Analysis of the data in Tables (1S–6S) (Supplementary materials) calculated for the bond lengths and angles for the bond, one can conclude the following remarks:

(1) The N(15)—N(16), C(13)—N(15), C(13)—O(14) and N(16)—C(17) azomethine bond lengths in ligand (1.368, 1.399, 1.224 and 1.023 Å) become largely longer in complexes(3.797, 3.114, 3.549 and 3.591 Å) as the coordination takes place via N atoms of —C=N—C=N— group that is formed on deprotonation of OH group in both $[Cu(A2PNA)_2]$-H_2O and $[Zn(A2PNA)(OAc)(H_2O)]$ complexes [31].
(2) The C(2)—O(4) bond distance in all complexes becomes longer due to the formation of the M—O bond which makes the C—O bond weaker [32].
(3) In $[Cu(A2PNA)_2]H_2O$ complex, C(4)—N(3) and C(26)—N(25) bond distances of the two pyridine rings pyridine are enlonged. This is referred to the formation of the M—O bond which makes the C—O bond weaker and forming a double bond character [33].
(4) The bond angles of the hydrazone moiety of HA2PNA are altered somewhat upon coordination; the largest change affects C(13)—N(15)—N(16) and O(14)—C(13)—N(15) angles which are reduced or increased on complex formation as a consequence of bonding [31].
(5) The C(13)—N(15)—N(16) angle in ligand changes from 119.8° to 92.1° or 116.6° in$[Cu(A2PNA)_2]H_2O$ and $[Zn(A2PNA)(OAc)(H_2O)]$ complexes due to the formation of the N(8)—Cu—O(13) and N(10)—Zn—O(14) chelate ring [31].
(6) The bond angles around the metal ion in $[Cu(A2PNA)_2]H_2O$ and $[Zn(A2PNA)(OAc)(H_2O)]$ complexes indicate that the complex adopts an octahedral arrangement predicting sp3 d^2 hybridization.
(7) The complexes can be arranged according to M—$N_{azomethine}$, M—$N_{pyridine}$ and M—O bond lenghts as follows: Zn(25)—N(16), Zn(25)—N(24)>Cu(49)—N(8)){or Cu(49)—N(33)}, Cu(49)—N(3), Cu(49)—N(25)and Zn(25)—O(14) > Cu(49)—O(13){or Cu(49)—O(37)} reflecting the great strength of the Cu—N and Cu—O bonds.
(8) The lower HOMO energy values show that molecules donating electron ability is the weaker. On contrary, the higher HOMO energy implies that the molecule is a good electron donor. LUMO energy presents the ability of a molecule receiving electron [33].
(9) The bond angles within the hydrazone backbone do not change significantly but the angles around the metal undergo appreciable variations upon changing the metal center [34].

IR spectra

The principle IR bands of HA2PNA and its metal complexes are listed in Table 2. The IR spectrum of HA2PNA (Structure I) showed two bands at 1695 and 1626 cm^{-1}, attributable to ν(C=O) and ν(C=N) [35], respectively. The bands observed at 1581 and 950 cm^{-1} are assigned to ν(C=N) pyridine [36] and pyridine ring breathing mode [37], respectively. The medium intensity band at 1153 cm^{-1} is attributed to ν(N—N) [38], while the band at 3201 cm^{-1} is assigned to the stretching NH group. The two medium intensity bands at 630 and 410 cm^{-1} are assigned to the pyridine ring deformation and in plane ring deformation and out of plane deformation [39,40].

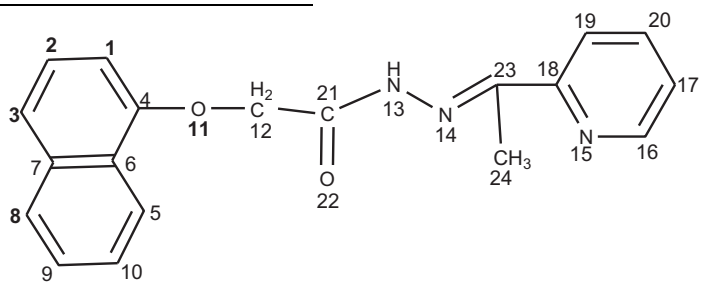

(*Z*)-2-(naphthalen-1-yloxy)-*N*'-(1-(pyridin-2-yl)ethylidene)acetohydrazide

(HA2PNA)

The IR spectra of $[Zn(A_2PNA)(OAc)(H_2O)]$ and $[Cu(A2PNA)_2]H_2O$ complexes (Structures II and III) show that HA2PNA acts as a mononegative tridentate ligand, coordinating via the deprotonated carbonyl oxygen (=C—O—) and both (C=N)imine and (C=N)pyridine nitrogen atom. This mode of chelation (Structures II and III) is confirmed by the following observations: (i) the disappearance of ν(C=O), ν(C=N)imine and ν(NH) [41] with simultaneous appearance of new bands in the range 1260–1270 and 1568–1588 cm^{-1} assignable to ν(C—O) and ν(—C=N—N=C—), respectively [42,43] (iii) ν(C=N)pyridine and pyridine ring breathing mode together with ν(N-N) shift to higher wavenumber, and (iv) the appearance of new bands in the regions 485–510 and 420–424 cm^{-1} assignable to ν(M—O) [44] and ν(M—N) [45], respectively.

Table 2
Most important IR spectral bands of HA2PNA and its metal complexes.

Compound	ν(NH)	ν(C=O)	ν(C=N)	ν(C=N)$_{pyridine}$	ν(C=N—N=C)	ν(C—O)	ν(N—N)	Pyridine ring breathing mode	ν(M—O)	ν(M—N)
HA2PNA	3201	1695	1626	1581	–	–	1153	950	–	–
$[Zn(A2PNA)(OAc)(H_2O)]$	–	–	–	1592	1569	1260	1153	954	488	420
$[Cu(A2PNA)_2]H_2O$	–	–	–	1599	1570	1265	1172	960	490	420

Table 3
Magnetic Moments, Electronic Bands and Ligand Field Parameters of Metal Complexes of HA2PNA.

Compound	Band position (cm^{-1})	Assignment transition	Ligand field parameters			μ_{eff} (B.M.)
			D_q (cm^{-1})	B (cm^{-1})	β	
HA2PNA	36231	$(\pi \rightarrow \pi^*)_{py}$	–	–	–	–
	33783	$(\pi \rightarrow \pi^*)_{C=N}$				
	29412	$(\pi \rightarrow \pi^*)_{C=N}$				
$[Cu(A2PNA)_2]H_2O$	14493	$^2B_{1g} \rightarrow {}^2E_g$	–	–	–	2.1
	17453	$^2B_{1g} \rightarrow {}^2A_{1g}$				

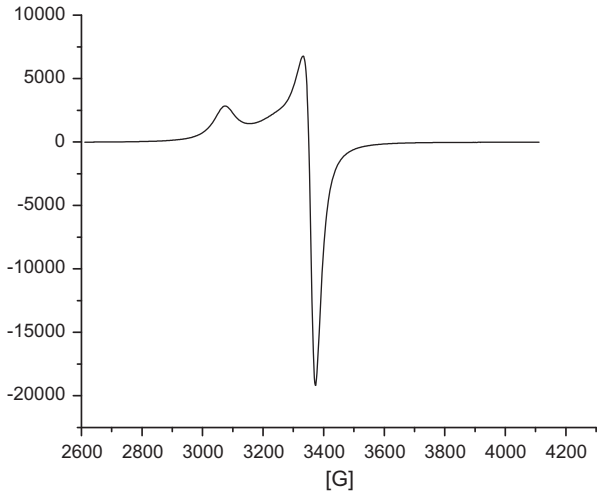

Fig. 1. X-band ESR spectrum of $[Cu(A2PNA)_2]\cdot H_2O$.

The ^1H NMR

^1H NMR spectrum of HA2PNA (Structure I) in DMSO-d6 showed signals at δ = 11.05 ppm (s, 1H), 5.02 (s, 2H), and 2.30 (s, 3H) ppm assignable to the, NH, CH2 and CH3 protons, respectively. The signal due to NH proton disappears upon adding D_2O. The signals due to pyridine ring protons appear at δ:8.62 ppm {(m, 2H, H—C16=H—C17, J = 7.50 Hz),(H=C16=H—C20. J = 1.5, H—C17=H=C16, J = 7.5 Hz)}, δ:8.50 ppm{(d, 2H, H=C19=H—C20, J = 7.5 Hz),: 8.2{2H, H=C17=H=C18)} and δ:7.80 ppm {(d, 2H, H=C20=H=C17, J = 7.5 Hz)},(H=C20=H=C19, J = 7.5 Hz)} [46]. On the other hand the signals due to naphthyl protons appear at δ:7.66 ppm{(dd, 2H, H=C10=H=C5, (H=C9=H=C10, J = 7.50, 1.50 Hz)}, δ:7.64{(dd, 2H, H=C9=H=C10, J = 7.50, 1.50 Hz), (H=C8=H=C9, J = 7.50, 1.50 Hz), δ:7.50 ppm{dd, H—C8=H=C7,H=C9=H=C8, J = 7.50 Hz)}; δ:7.42 ppm{(dd, 2H, H=C1=H=C2), (H=C1=H=C3, J = 7.50, 1.50 Hz), δ:7.40 ppm {(dd, 2H, H—C3=H=C2,),(H=C2=H=C3, J = 7.50, 1.50 Hz) and δ:6.90 ppm {(dd, 2H, H=C1=H=C2,),(H=C1=H—C3, J = 7.50, 1.50 Hz), respectively.

Electronic spectra and magnetic measurements

The UV–visible spectral bands of the HA2PNA and its complexes in DMSO or Nujol mull as well as the magnetic moments and the ligand field parameters are recorded in Table 3. The electronic spectra of the complexes are dominated by intense intra-ligand charge transfer bands. The spectrum of the ligand shows an intense absorption band at 364231 cm^{-1} assignable to $\pi \rightarrow \pi^*$ transition of pyridine ring. A red shift is observed for this transition in the spectra of complexes as a result of coordination of the nitrogen of the pyridine ring [46]. Another intense absorption band in the region 33783 cm^{-1} is due to $\pi \rightarrow \pi^*$ transition of C=N group which shifts in complexes toward higher frequencies, supporting the coordination of the hydrazone via azomethine nitrogen atom. A third intense band appears at 29411 cm^{-1} assignable to $n \rightarrow \pi^*$ transition of carbonyl group [47]. In $[Cu(A2PNA)_2]H_2O$ complex, the bands are shifted by 150–409 cm^{-1}. The electronic spectrum of the complex shows two bands at 14493 and 17543 cm^{-1} attributed to $2B_{1g} \rightarrow 2E_g$ and $2B_{1g} \rightarrow 2A_{1g}$ transitions, respectively, in an octahedral geometry. The magnetic moment value of the Cu(II) complex (2.1 B.M.) lies within the range of Cu(II) ions in a d^9 system [48].

Electron spin resonance

ESR spectra of Cu(II) complex provide s information about hyperfine and super hyperfine structures which are important in studying the metal ion environment in the complexes, i.e. the geometry, nature of the ligation sites from the Schiff bases of the metal and the degree of covalency of the metal- ligand bonds (Fig. 1).The spin Hamiltonian parameters of the complexes with Cu(II), S = 1/2, I = 3/2, were calculated and are summarized in Table 4.

The room temperature solid state ESR spectra of the $[Cu(A2PNA)_2]H_2O$ complex exhibits an axially symmetric g-tensor parameters with $g_{||} > 2.0023$ indicating that the copper site has a $dx^2 - y^2$ ground-state characteristic of square planar or octahedral stereochemistry [49]. In axial symmetry, the g-values are related by the expression, $G = (g_{||}/-2)/(g_{\perp}-2) = 4$. According to Hathaway [50], as value of G is greater than 4, the exchange interaction between copper (II) centers in the solid state is negligible, whereas when it is less than 4, a considerable exchange interaction is indicated in the solid complex. The calculated G value for the copper complex is less than 4 suggesting copper–copper exchange interactions. A forbidden magnetic dipolar transition for the Cu(II) complex is observed at half-field (ca. 16000 G, $g \approx 4.0$) but the intensity is very weak. The tendency of $A_{||}$ to decrease with concomitant increase of $g_{||}$ is an index of an increase of the tetrahedral distortion in the coordination sphere of copper. In order to quantify the degree of distortion of the Cu(II) complex, the we selected the $f(\alpha) = g_{||}/A_{||}$ obtained from the ESR spectra which is regarded as an index of tetrahedral distortion. Values of $f(\alpha)$:110–120 are typical for planar complexes, while the range of 130–150 is characteristic of slight to moderate distortion and 180–250 cm^{-1} indicates considerable distortion [51,52]. The ratio $g_{||}/A_{||}$ for the present complex is 177 demonstrating the presence of significant dihedral angle

Table 4
ESR data of the some Cu(II) complex at room temperature.

Complex	$g_{||}$	$g_{\perp}$	$A_{||} \times 10^{-4}$ cm^{-1}	G	$g_{||}/A_{||}$	α^2	β^2
$[Cu(HA_2PNA)_2]H_2O$	2.247	2.067	126.37	3.63	177.00	0.49	0.68

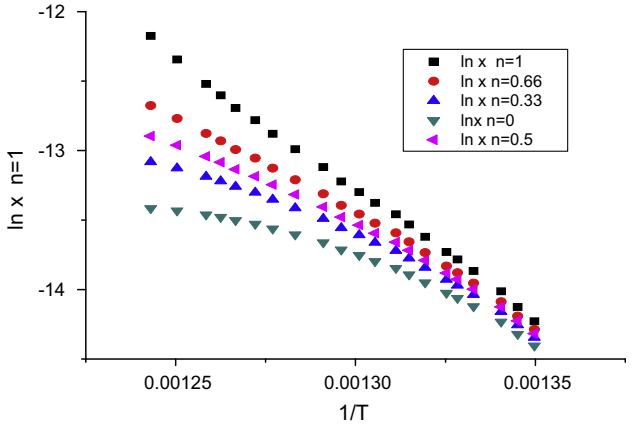

Fig. 2a. Coats–Redfern plot of first degradation step $[Cu(A2PNA)_2]H_2O$ complex.

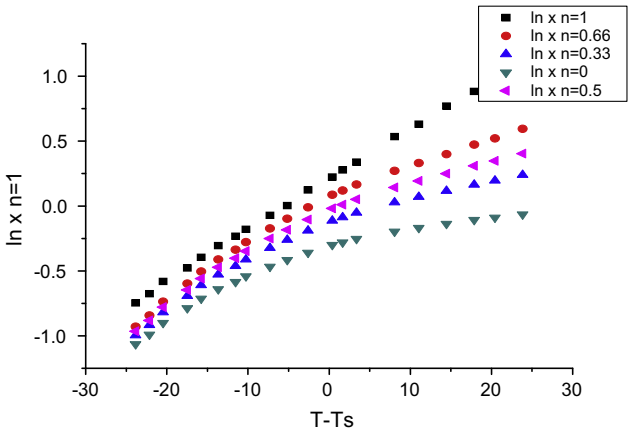

Fig. 2b. Horowitz–Metzger plot of first degradation step for $[Cu(A2PNA)_2]H_2O$.

distortion in the *xy*-plane and the results are consistent with distorted octahedral geometry around the copper site. The molecular orbital coefficients, α^2 (A measure of the covalency of the in-plane σ-bonding between a copper 3d orbital and the ligand orbitals) and β^2 (covalent in-plane π-bonding), were calculated by using the following equations [53–56].

$$\alpha^2 = (A||/0.036) + (g|| - 2.0023) + 3/7(g \perp -2.0023) + 0.04$$

$$\beta^2 = (g|| - 2.0023)E/ - 8\lambda\alpha 2$$

where $\lambda = -828\ cm^{-1}$ for the free copper ion and E is the electronic transition energy.

As a measure of the covalency of the in-plane σ-bonding $\alpha^2 = 1$ indicates complete ionic character, whereas $\alpha^2 = 0.5$ denotes 100% covalent bonding, with the assumption of negligibly small values of the overlap integral. The β^2 parameter gives an indication of the covalency of the in-plane π-bonding. The smaller the β^2, the larger the covalency of the bonding.

The values of α^2 and β^2 for Cu(II) complex indicates that the in-plane σ-bonding and in-plane π-bonding are covalent which originate from the fact that imine binding in the complex incorporates greater covalency in the metal–ligand bonding through delocalized $d_\pi - P_\pi$ in-plane π-bonding as evidenced from higher β^2 values [57]. On the other hand, the data for $[Cu(HAPO)Cl](H_2O)$ complex, shows that the in-plane σ-bonding and in-plane π-bonding are appreciably ionic. These results are anticipated because there are appropriate ligand orbitals to combine with the dxy orbital of the Cu(II) ion. For the square planar geometry complexes, the lower values of β_2 compared to α_2 indicate that the in-plane π-bonding is more covalent than the in-plane σ-bonding. These data are well consistent with other reported values [58–60].

Thermogravimetric studies

The stages of decomposition, temperature range, decomposition product as well as the weight loss percentages of complexes are given in Table 7S (Supplementary materials). One of the features in TGA data concerning the associated water or coordinated molecules within the complexes supporting the elemental analyses. Fig. 1S (Supplementary material) shows the TGA curve of $[Cu(A2PNA)_2]H_2O$ complex as a representative example which displays three degradation steps. The first step at 35–100 °C with weight loss of 11.90 (Calcd. 11.68%) is attributed to the loss of one lattice water molecule. The second step with weight loss of 39.59 (Calcd. 39.09%) at 210–332 °C is corresponding to the removal of two naphthyl moiety. The third step at 391–557 °C with weight loss of 33.83 (Calcd. of 34.86%) is referring to the removal of 2 pyridyl + 2 $OCH_2 + N_2$ fragements. The residual part is $CuO + 2C + C_6H_6O$ (Found 22.34, Calcd. 24.79%).

Kinetic data

In order to assess the influences of the structural properties of the chelating agent and the type of the metal on the thermal behavior of the complexes, the order (n) and the heat of activation E_a of the various decomposition stages were determined from the TG and DTG using the Coats–Redfern [61] and Horowitz–Metzger [62] (Fig. 2). The obtained data were in Tables 5 and 6. The rate of thermal decomposition of a solid $(\frac{d\alpha}{dt})$ expressed by the Arrhenius equation has the following form:

$$\frac{d\alpha}{dt} = A\exp\left(-\frac{E_a}{RT}\right)g(\alpha) \quad (1)$$

where E_a is the activation energy, A is the Arrhenius pre-exponential factor, R is the gas constant and $g(\alpha)$ is the differential conversion factor and equal $(1-\alpha)n$ where n is the reaction order, assumed to remain constant during the reaction[63,64]. A large number of decomposition processes can be represented as first order reaction [65], particularly, the degradation of the investigated series of metal complexes. Under this assumption the integration of Eq. (1) leads to:

$$\ln(1-\alpha) = -\frac{A}{\beta}\int_{T_o}^{T}\mathrm{Exp}\left(-\frac{E_a}{RT}\right)dT \quad (2)$$

Table 5
Kinetic parameters evaluated by Coats–Redfern equation for HA2PNA metal complexes.

Complex	Peak	Mid temp (K)	E_a (kJ/mol)	A (S^{-1})	ΔH^* (kJ/mol)	ΔS^* (kJ/mol K)	ΔG^* (kJ/mol)
$[[Cu(A2PNA)_2]H_2O$	1st	349.52	8.06	5.71×10^3	35.16	−0.1743	96.08
	2nd	536.94	83.18	1.34E + 06	78.72	−0.1325	149.88
	3rd	772.67	153.34	2.04E + 08	146.92	−0.0937	219.35
$[Zn(A2PNA)(OAc)(H_2O)]$	1st	612.88	208.73	9.72E + 15	203.63	0.0552	169.82
	2nd	675.39	374.12	2.57E + 27	368.50	0.2730	184.12
	3rd	1021.19	487.09	1.01E + 23	478.60	0.1852	289.44

Table 6
Kinetic Parameters evaluated by Horowitz–Metzger equation for HA_2PNA complexes.

Complex	Peak	Mid Te p (K)	E_a kJ/mol	A (S^{-1})	ΔH^* (kJ/mol)	ΔS^* (kJ/mol K)	ΔG^* (kJ/mol)
$[Cu(A2PNA)_2]H_2O$	1st	349.52	17.01	6.81×10^3	ΔH^*	−0.1753	98.08
	2nd	536.94	92.42	1.16E + 07	kJ/mol	−0.1146	149.47
	3rd	772.67	166.72	1.76E + 09	35.66	−0.0759	218.90
$[Zn(A2PNA)(OAc)(H_2O)]$	1st	612.88	219.24	7.97E + 16	87.95	0.0727	169.61
	2nd	675.39	385.35	1.93E + 28	160.29	0.2898	184.01
	3rd	1021.19	505.07	8.63E + 23	214.14	0.2031	289.20

Table 7
Anti-inflammatory effect and analgesic effect of Piroxicam, $[Cu(AC)_2]\cdot 2H_2O$, $Zn(Ac)_2]\cdot 2H_2O$ HA2PNA, $[Cu(A2PNA)_2]H_2O$ complex and $[Zn(A2PNA)(OAc)(H_2O)]$ complex in Collagen II – Freund's adjuvant induced rheumatoid arthritis in rats ($n = 6$, M ± S.E).

Group	Dose (mg/200 g of rat weight)	Rheumatoid index	Analgesic effect	
			Pain tolerance	Pain scoring
Non-arthritic non-treated	[SCMC] Solvent	1.00 ± 0.00	12.50 ± 0.56	1.00 ± 0.00
Arthritic non-treated	[SCMC] Solvent	3.88 ± 0.19[a]	3.92 ± 0.30[a]	3.83 ± 0.17[a]
Piroxicam	0.36	2.55 ± 0.21[a, b]	5.79 ± 0.15[a, b]	2.43 ± 0.19[a, b]
$[Cu(AC)_2]\cdot 2H_2O$	0.22	3.4 ± 0.29 [a]	4.51 ± 0.37 [a]	3.32 ± 0.26 [a]
$Zn(Ac)_2]\cdot 2H_2O$	0.22	3.53 ± 0.29 [a]	4.49 ± 0.18 [a]	3.24 ± 0.12 [a]
HA2PNA	0.36	1.53 ± 0.1 [b, c, d, e]	7.82 ± 0.41[a, b, c, d, e]	1.41 ± 0.11 [b, c, d, e]
$[Cu(A2PNA)_2]H_2O$	0.96	1.47 ± 0.11 [b, c, d, e]	8.11 ± 0.45[a, b, c, d, e]	1.23 ± 0.13 [b, c, d, e]
$[Zn(A2PNA)(OAc)(H_2O)]$	0.97	1.42 ± 0.13 [b, d, e]	7.93 ± 0.45[a, b, c, d, e]	1.32 ± 0.12 [b, c, d, e]

SCMC 0.5% sodium carboxymethyl cellulose.
Θ $P < 0.01$ vs. HA2PNA.
[a] $P < 0.001$ vs. non-arthritic control.
[b] $P < 0.01$ vs arthritic control.
[c] $P < 0.01$ vs. piroxicam.
[d] $P < 0.01$ vs. $[Cu(AC)_2]\cdot 2H_2O$.
[e] $P < 0.01$ vs. $Zn(Ac)_2]\cdot 2H_2O$.

On the basis of Eq. (2), it is possible to analyze experimental data by the integral method, in order to determine the degradation kinetic parameters A, E_a.The other thermodynamic parameters of activation can be calculated by Eyring equation [66,67].

From the results obtained, all decomposition steps show best fit for $n = 1$ and the negative value of ΔS^*(entropy of activation) of some decomposition steps indicates that the activated fragments have more ordered structure than the undecomposed ones and the later are slower than the normal [68,69]. The positive sign of ΔH^* (activation enthalpy change) indicates that the decomposition stages are endothermic processes. The high values of E_a of the complexes reveal the high stability of such chelates due to covalent bond between central metal ion and the hetero atom of the ligand [70]. The positive sign of ΔG^* for the investigated complexes reveals that the free energy of the final residue is higher than that of the initial compound, and hence all the decomposition steps are non-spontaneous processes.

Results and discussion: Pharmacology

Anti-inflammatory effect

Animal treatment by piroxicam, (HA2PNA), Cu(II) and Zn(II) ligand complex induced a significant anti-inflammatory effect detectable by the 7th day big joint inflammation as compared with that of the arthritic non-treated group (Table 7). Moreover, HA2PNA, Cu(II) and Zn(II) complexes treated group showed a significant decrease in Rheumatoid index by the 7th day versus piroxicam treated group (Table 7). The anti-inflammatory, analgesic and antipyretic activity of piroxicam is through inhibition of prostaglandin synthetase, via inhibition of cyclooxygenase enzymes [4].

The anti-inflammatory effects of copper and zinc have been documented in animals [71] and in humans [9]. Copper and zinc are constituents of the superoxide-dismutase (SOD) enzyme, which performs intracellular antioxidant functions [72]. Also, Copper is a constituent of ceruloplasmin, a powerful extracellular antioxidant enzyme [73].

The anti-inflammatory activity of Cu-complexes is due to the physicochemical properties of the complex rather than its constituents [74]. There are several possible mechanisms for the anti-inflammatory activity of copper complexes. The copper may induce lysyl oxidase activity [75], decrease the permeability of human synovial lysosomes [76], modulate the physiological effects of histamine [77] and a number of copper(II) complexes have been reported to exhibit SOD-mimic activity and thus are viewed as alternative therapeutics to remove pro-inflammatory superoxide anion radical in vivo [78,79]. Also, Copper induces an inhibition of PGE2 synthetase leading to a shift in synthesis from the inflammatory PGE2 to anti-inflammatory PGF series [80].

The analgesic effect

The pain score was decreased and pain tolerance was increased by the 7th day in the treated groups with piroxicam, ligand (HA2PNA), Cu(II) complex and Zn(II) complex as compared with that of the arthritic non-treated group (Table 7). It is worth noting that HA2PNA, Cu(II) complex and Zn(II) complex showed a better activity in reducing pain score and increasing pain tolerance than of piroxicam (Table 7). [81] Presented similar results for naproxen in the model of abdominal writhing induced by acetic acid in mice and demonstrated that zinc–naproxen had a greater antinociceptive effect in the abdominal writhing induced by acetic acid and in the tail-flick test than naproxen alone at the same concentration [81]. Zinc alleviates pain through high-affinity binding to the NMDA receptor NR2A subunit [82]. our results differ from those reported by Santos et al. (2004) who demonstrated that zinc–diclofenac complex in rats does not change the antinociceptive effect of diclofenac [83]. Also, similar to our results complexation of NSAIDs with copper produced more potent analgesic agents [84]. The

enhanced analgesic activity of Copper complexes can be explained by activation of copper-dependent opioid receptors [85]. Up to our knowledge, Literature survey showed no pharmacological assay on the present hydrazone, 2-acetylpyridine-α-naphthoxyacetylhydrazone (HA2PNA) and the precise molecular mechanism(s) of its anti-inflammatory and analgesic effects discovered in the present study need further investigations to be explained.

Conclusion

New Cu(II) and Zn(II) complexes of 2-(naphthalen-1-yloxy)-*N*′-(1-(pyridin-2-yl)ethylidene) acetohydrazide (HA2PNA) have been prepared and characterized by conventional measurements. The data revealed an octahedral geometry of the metal complexes. Also, the thermal behavior of the solid metal complexes and the corresponding kinetic parameters were evaluated using Coats–Redfern and Horowitz–Metzger methods. Moreover, the ligand and its complexes were screened for anti-inflammatory and analgesic activity in rat model of collagen adjuvant arthritis and compared with piroxicam. All the compounds showed a higher activity of their reducing pain score and increasing pain tolerance than of piroxicam. The enhanced analgesic activity of Copper complexes may be explained by activation of copper-dependent opioid receptors and that of Zinc alleviates pain through high-affinity binding to the NMDA receptor NR2A subunit. However the precise molecular mechanism(s) of the anti-inflammatory and analgesic effects discovered in the present study need further investigations to be explained.

Appendix A. Supplementary material

Supplementary data associated with this article can be found, in the online version, at http://dx.doi.org/10.1016/j.saa.2013.09.067.

References

[1] D. Aletaha, T. Neogi, A.J. Silman, J. Funovits, D.T. Felson, Ann. Rheum. Dis. 69 (2010) 1580.
[2] C. Grigor, H. Capell, A. Stirling, A.D. McMahon, P. Lock, R. Vallance, Lancet 364 (2004) 263.
[3] G. Dannhardt, W. Kiefer, Eur. J. Med. Chem. 36 (2001) 109.
[4] I.F. Abdallah, H.M. Dawaba, A. Mansour, A.M. Samy1, Inter. J. Pharm. Pharm. Sci. 3 (2011) 975.
[5] B.C. Starcher, C.H. Hill, J.G. Madaras, J. Nutr. 110 (1980) 2095.
[6] R. Lappalainen, M. Knuuttila, S. Lammi, E.M. Alhava, H. Olkkonen, Acta Orthop. Scand. 53 (1982) 51.
[7] P.J. Fraker, P. Jardieu, J. Cook, Arch. Dermatol. 123 (1987) 1699.
[8] J.R. Stabel, J.W. Spears, Adv. Exp. Med. Biol. 258 (1989) 243.
[9] R. Milanino, A. Frigo, L.M. Bambara, M. Marrella, U. Moretti, M. Pasqualicchio, Clin. Exp Rheum. 11 (1993) 271.
[10] S. Ala, M. Shokrzadeh, A.M. Pur Shojah, S.S. Saeedi Saravi, Pak., J. Biol. Sci. 12 (2009) 1041.
[11] G.E. Jackson, P.M. May, D.R. Williams, J. Inorg. Nucl. Chem. 40 (1978) 1189.
[12] S. Rollas, Ş.G. Küçükgüzel, Molecules 12 (2007) 1910.
[13] P. Vicini, M. Incerti, I.A. Doytchinova, P. La Colla, B. Busonera, R. Loddo, Eur. J. Med. Chem. 41 (2006) 624.
[14] H.J.C. Bezerra-Netto, D.I. Lacerda, A.L.P. Miranda, H.M. Alves, E.J. Barreiro, C.A.M. Fraga, Bioorg. Méd. Chem. 4 (2006) 7924.
[15] G.P. Pokhariyal, B. Lai, V.K. Rastogi, Asian J. Chem. 9 (1997) 541.
[16] K. Gewald, I. Hofmann, J. Prakt. Chem. 311 (1969) 402.
[17] W.J. Geary, Coord. Chem. Rev. 7 (1971) 81.
[18] M.N. Ghosh, H.O. Schild, Fundamentals of Experimental Pharmacology, 1st ed., Scientific Book Agency, Calcutta, 1971. pp. 84.
[19] D.E. Trentham, A.S. Townes, A.H. Kang, J. Exp Med. 146 (1977) 857.
[20] R. Halmdahal, V. Malmstrom, V.E. Vuorio, Annul. Med. 25 (1993) 251.
[21] B.H. Waksman, C.M. Person, J.T. Sharp, J. Immunol. 85 (1960) 403.
[22] F.D. Wood, G.M. Pearson, N. Tankan, Int. Arch. Allergy. 35 (1969) 456.
[23] L.O. Randall, J.J. Selitto, Arch. Intl. Pharmacol. 111 (1957) 409.
[24] -J.R. Ward, R.S. Jones, Arthr. Rheum. 5 (1962) 557.
[25] B. Delley, Phys. Rev. 65 (2002) 85403.
[26] Materials studio v 5.0, copyright Accelrys software Inc., 2009.
[27] W.J. Hehre, L. Radom, P.V.R. Schlyer, J.A. Pople, Ab Initio Molecular Orbital Theory, Wiley, New York, 1986.
[28] A. Kessi, B. Delley, Int. J. Quant. Chem. 68 (1998) 135.
[29] B. Hammer, L.B. Hansen, J.K. Nørskov, Phys. Rev. B 59 (1999) 7413.
[30] A. Matveev, M. Staufer, M. Mayer, N. Rösch, Int. J. Quant Chem. 75 (1999) 863.
[31] O.A. El-Gammal, Spectrochim. Acta A 75 (2010) 533.
[32] D.X. West, J.K. Swearingen, J. Valdés-Martinez, S. Hernández-Ortega, A.K. El-Sawaf, F.v. Meurs, A. Castiñeiras, I. Garcia, E. Bermejo, Polyhedron 18 (1999) 2919.
[33] A.A.R. Despaigne, J.G.D. Silva, A.C.M.D. Carmo, O.E. Piro, E.E. Castellano, H. Beraldo, J. Mol. Struct. 920 (2009) 97.
[34] S. Sagdinc, B. Koksoy, F. Kandemirli, S.H. Bayari, J. Mol. Struct. 917 (2009) 63.
[35] S.Y. Chundak, V.M. Leovac, D.Z. Obadeovic, D.M. Petrovic, Transation Met. Chem. 11 (1986) 308.
[36] S. PPerlepes, D. Kovola-Demertzi, S. Skaribas, D. Nicholls, S. Paraskevas, Thermochim. Acta. 147 (1989) 153.
[37] T.H. Rakha, M.M. Bekheit, Chem.Pharm.Bull. 48 (2000) 914.
[38] T.H. Rakha, Synth. React. Inorg. Met-Org. Chem. 30 (2000) 205.
[39] D.P. Madam, M.M. da Mota, S.M. Nelson, J. Chem. Soc. A 40 (1970) 90.
[40] D.P. Madam, M.M. da Mota, S.M. Nelson, J. Chem. Soc. A 40 (1968) 2342.
[41] M.F. El-Shazly, L.S. Refaat, Trans. Met. Chem. 8 (1981) 8.
[42] F.A. El-Saied, A.M. Donia, S.M. Hamza, Thermochim. Acta 189 (1991) 297.
[43] C. Lorenzini, C. Pelizzi, G. Predieri, J. Chem. Soc. Dalton Trans. (1983) 721.
[44] A.N. Speca, N.M. Karayanis, L.L. Pytlewski, Inorg. Chim Acta 9 (1974) 87.
[45] B. Beecroft, M.J.M. Campbell, Grzeskowia, J. Inorg. Nucl. Chem. 36 (1974) 55.
[46] R. Tamara, U. Todorović, B. Rychlewska, B. War_ zajtis, D.D. Radanović, N.R. Filpovic, I.A. Pajic, D.M. Sladic, K.K. Andelkovic, Polyhhedron. 28 (2009) 2397.
[47] M. Mohan, M. Kumar, Trans. Met. Chem. 10 (1985) 255.
[48] J. Chakraborty, S. Thakurta, G. Pilet, D. Luneau, S. Mitra, Polyhedron 28 (2009) 819.
[49] S. Delgado, M. Moran, U. Fernandez, J. Coord. Chem. 12 (1982) 105.
[50] B.J. Hathaway, D.E. Billing, Coord. Chem. Rev. 5 (1970) 143.
[51] A.W. Addison, in: K.D. Karlin, J. Zubieta (Eds.), Spectroscopic and Redox Trends From Model Copper Complexes, Adenine Press, New York, 1983.
[52] V.V. Pavlischuk, Theor. Exp. Chem. 1 (1995) 31.
[53] R.K. Ray, G.R. Kauffman, Inorg. Chem. Acta 207 (1990) 173.
[54] K. Jayasubramanian, S.A. Samath, S. Thambidurai, R. Murugesan, S.K. Ramalingam, Trans. Met. Chem. 20 (1995) 76.
[55] V.S.X. Anthonisamy, R. Murugesan, Chem. Phys. Lett. 287 (1998) 353.
[56] V.S.X. Anthonisamy, R. Anantharam, R. Murugesan, Spectrochim. Acta A 55 (1999) 135.
[57] N. Raman, Y.P. Raja, A. Kulandaisamy, Proc. Ind. Acad. Sci. 113 (2001) 183.
[58] R.P. John, Spectrochim. Acta A 59 (2003) 1349.
[59] G.A.A. Al-Hazmi, M.S. El-Shahawi, E.M. Gabr, A.A. El-Asmy, J. Coord. Chem. 58 (2005) 713.
[60] O.A. El-Gammal, G.M. Abu El-Reash, S.E. Ghazy, T. Yousef, J. Coord. Chem. 65 (2012) 1655.
[61] W. Coats, J.P. Redfern, Nature 201 (1964) 68.
[62] H.H. Horowitz, G. Metzger, Anal. Chem. 35 (1963) 1464.
[63] M.S. Abu-Bakr, H. Sedaira, E.Y. Hashem, Talanta 41 (1994) 1669.
[64] D. Kara, M. Alkan, Talanta 55 (2001) 415.
[65] A. Broido, J. Polym. Sci. A-2 7 (1969) 1761.
[66] K. Schwetlick, "Kinetyczne Metody Badania Mechanizmow Reakcji", PWN Warszawa, 1975.
[67] R.G Mortimer, Physical Chemistry Harcourt and Science Technology Company, Academic Press, San Diego, 2000.
[68] S.H. Guzar, Q.H. Jin, Chem. Res. Chin. Univ. 24 (2008) 143.
[69] H.T.S. Britton, Hydrogen Ions, 3rd ed., Chapman and Hall, London, 1942.
[70] T. Taakeyama, F.X. Quinn, Thermal Analysis Fundamentals and Applications to Polymer Science, John Wiley and Sons, Chichester, 1994.
[71] R. Milanino, U. Moretti, M. Concari, M. Marrella, G.P. Velo, Agents Actions 24 (1988) 365.
[72] S. Tuncer, A. Kamanli, E. Akcil, G.O. Kavas, B. Seckin, M.B. Atay, Biol. Trace Elem. Res. 68 (1999) 137.
[73] B. Halliwell, J.M.C. Gutteridge, Arch. Biochem. Biophys. 28 (1990) 1.
[74] J.R.J. Sorenson, Metal/Ligand Interactions in Biological Fluids, 1st ed., Marcel Dekker, New York, 1995 (vol. 2).
[75] E.D. Harris, Proc. Natl. Acad. Sci. USA 73 (1976) 371.
[76] J. Chayen, L. Bitensky, R.G. Butcher, L.W. Poulter, Nature 222 (1969) 281.
[77] J.R. Sorenson, in: G.P. Ellis, G.B. West (Eds.), Progress in Medicinal Chemistry, vol. 15, Elsevier, Amsterdam, 1978, p. 211.
[78] S. Ahmad, Oxidative Stress and Antioxidant Defenses in Biology, 1st ed., Chapman & Hall, New York, 1995.
[79] M. Gonzalez-Alvarez, G. Alzuet, J. Borras, L.A. del Castillo, J.M. Montego-Bernado, S. Garcia-Granda, J. Biol. Inorg. Chem. 8 (2003) 112.
[80] M.E. Elmes, Lancet 304 (1974) 1329.
[81] Jain NK, S. Amarjit, S.K. Kulkarni, Pharm. Pharm. Commun. 5 (1999) 599.
[82] C. Nozaki, A.M. Vergnano, D. Filliol, Abdel-Mouttalib Ouagazzal, A.L. Goff, S. Carvalho, D. Reiss, C. Gaveriaux-Ruff, J. Neyton, P. Paoletti, B.L. Kieffer, Nat. Neurosci. 14 (2011) 1017.
[83] L.H. Santos, C.A.O. Feres, F.H. Melo, M.M. Coelho, M.S. Nothenberg, S. Oga, C.A. Tagliati, Braz. J. Med Biol. Res., 8 (2004) 7.
[84] F. Gumilar, M. Agotegaray, C. Bras, N.A. Gandini, A. Minetti, Eur. J. Pharmacol. 675 (1–3) (2012) 32–39.
[85] S. Okuyama, S. Hashimoto, H. Aihara, W.M. Willingham, J.R. Sorenson, Agents Actions 21 (1987) 130.